Photoconductivity Enhancement in Multilayers of CdSe and CdTe Quantum Dots

Elise Talgorn, Marnix A. de Vries, Laurens D. A. Siebbeles, and Arjan J. Houtepen*

Department of Chemical Engineering, Delft University of Technology, Julianalaan 136, 2628 BL Delft, The Netherlands

ABSTRACT Charge separation at the interface between CdSe and CdTe quantum dots was investigated by comparing the photoconductivity of films consisting of only CdSe or CdTe quantum dots to that of films with alternating layers of CdSe and CdTe quantum dots. The photoconductivity for alternating layers is three times higher than for the single component layers. Different possible mechanisms are discussed, and it is concluded that the dissociation of photoexcited excitons into spatially separated mobile charge carriers at the CdSe/CdTe QD interfaces is the most likely explanation. Given that the yield of charge carrier photogeneration in the multilayer sample is at most one, and under the assumption that the mobility of QD layers in unchanged, we conclude that the yield of charge carrier photogeneration in the single component samples is at most one-third. The thickness of the individual CdSe and CdTe layers was varied, resulting in different distances between the CdSe/CdTe interfaces. The photoconductivity increased with respect to films of only CdSe or CdTe when these interfaces were separated by only one or two quantum dot layers, which implies that exciton diffusion is inefficient.

KEYWORDS: quantum dots · CdSe · CdTe · photoconductivity · charge separation

Semiconductor nanoparticles, also called quantum dots (QDs), could be the new building blocks for cheap and efficient solar cells. Quantum confinement of charge carriers in QDs results in a size-dependent bandgap energy, allowing a flexible solar cell design.[1−3] Furthermore, quantum dots can be prepared in a relatively cheap, solution-based manner and have versatile surface properties.[4−6] The basic processes in a solar device are light absorption, charge separation, and charge transport. The large absorption coefficient and the tunable bandgap in QDs clearly allow optimization of light absorption.[7−10] Charge transport in films of QDs has been extensively studied, and it has been shown that short interparticle distances provide charge carrier mobilities sufficient for device applications.[11−18] Finally, operational solar devices require spatial separation of electrons and holes, which can be achieved by putting the QDs into contact with a wide-bandgap semiconductor material,[19,20] conjugated organic molecules,[21] or by means of a Schottky contact.[22] An "all-nanocrystal" option is to create a charge separating interface between two types of QDs. Films composed of CdSe and CdTe QDs could provide such an interface: CdSe and CdTe are reported to form a type II junction, where the difference in chemical potential drives the electrons toward CdSe and the holes toward CdTe.[23,24] A solar cell with a 3% power conversion efficiency consisting of sintered CdSe and CdTe QDs has supported this scheme.[23] In another study, charge separation between layers of CdSe and CdTe QDs has been evidenced by surface photovoltage spectroscopy.[24] In a junction consisting of QDs only, control over the energy levels of electrons and holes allows optimization of the offset between the levels of the different QDs and electrode materials. The voltage drops resulting from these level offsets could be minimized while keeping a flexible cell design.

Efficient charge separation in films of QDs still requires more understanding of the nature and dynamics of the primary photoexcitations. The extent to which photogenerated electron−hole pairs yield mobile charges in films of QDs is uncertain. Particularly, in cadmium chalcogenides, the exciton binding energy can be as high as ∼100 meV.[25] Inefficient screening of the electron−hole Coulomb interaction could result in a low charge carrier photogeneration yield.

In this paper, we report on the photogeneration of mobile charge carriers at an interface between CdSe and CdTe QDs in films of coupled QDs. We measured the photoconductivity of alternating layers of CdSe and CdTe QDs (from here on called *multilayer films*) separated by short linker molecules (1,2-ethanediamine) and compare it with that of single component CdSe and CdTe QD films. The thickness of the CdSe and CdTe QD *sublayers* within the multilayer films, that is, the distance between the CdSe/CdTe interfaces, was varied.

* Address correspondence to A.J.Houtepen@tudelft.nl.

Received for review November 2, 2010 and accepted April 25, 2011.

Published online April 25, 2011
10.1021/nn2009134

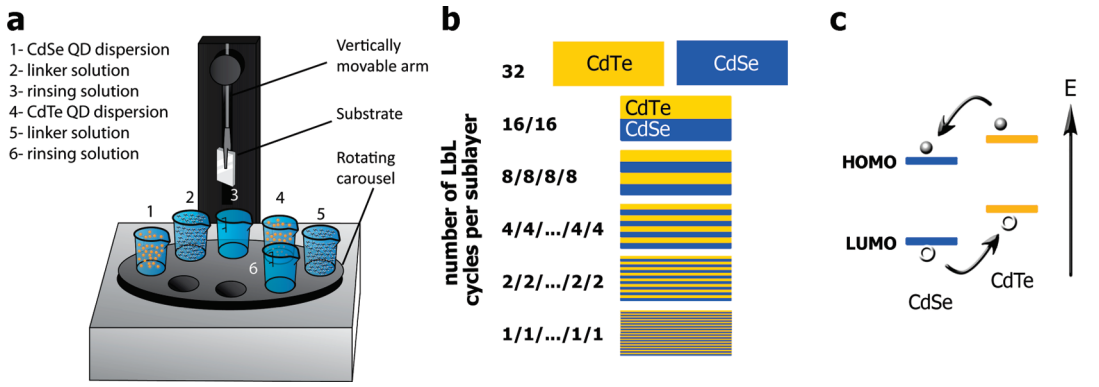

Figure 1. (a) Schematic of the automatic dip-coater and the solutions (numbered from 1 to 6) used for the LbL growth. One LbL cycle consists of dipping the substrate in solutions 1, 2, and 3 for depositing CdSe QDs or solutions 4, 5, and 6 for depositing CdTe QDs. (b) Schematic of the multilayer films with different number of LbL cycles per sublayer. All films consist of 32 LbL cycles in total. (c) Presumed energy band alignment for CdSe and CdTe QDs.

In the multilayer films where the sublayers are composed of only 1−2 QD monolayers, excitons are generated in a QD which is in contact with a QD of another type and can dissociate into free charges, resulting in an increase of the photoconductivity by a factor of 3 compared with that of single component films. For larger sublayer thicknesses no enhancement is observed. We discuss several mechanisms that could explain these observations and conclude that the most likely explanation is that photoexcitation predominantly results in bound excitons, which separate into mobile electrons and holes at the CdSe/CdTe interfaces. These excitons have a very short diffusion length corresponding to the length of 1−2 QDs only. We conclude that in the single component CdSe and CdTe QD films the yield of charge carrier photogeneration is at most one-third.

RESULTS AND DISCUSSION

Figure 1a schematically shows the investigated QD films, which were prepared with a layer-by-layer (LbL) technique.[15,26] The LbL technique allows the growth of smooth, glassy QD films,[15,26] wherein the long ligands that are originally present at the surface of the QDs are replaced by shorter molecules. A LbL cycle consists of the successive dipping of a substrate in a QD dispersion, a solution containing short linker molecules, and a rinsing solution (see Figure 1a and Experimental Section for details). This operation is repeated until the desired film thickness is attained. Here we use 1,2-ethanediamine (EDA, ~0.4 nm long[27,28]) as the replacement molecule as it has been shown previously to result in a significant electronic coupling between QDs.[15] EDA is a bidendate molecule; however, it is uncertain to which extent the deposition of the successive QD layers during the LbL process is mediated by binding of the QDs *via* the EDA molecules.[26] A detailed study on this LbL deposition approach can be found in ref 26. Single component films of CdSe or CdTe QDs and multilayer films consisting of alternating

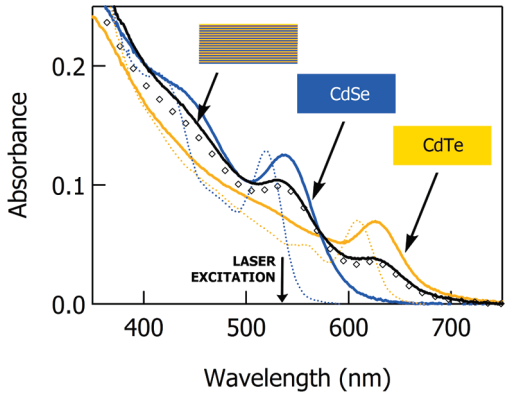

Figure 2. Absorption spectra of single component CdSe (blue solid curve) and CdTe (yellow solid curve) QD films and a multilayer film (black solid curve) composed of sublayers of 1 LbL cycle each. All films consist of 32 LbL cycles. The diamonds represent the average of the single component film absorbances. The absorption spectra of the QDs dispersed in solution are also shown (blue dotted curve for CdSe and yellow dotted curve for CdTe).

CdSe and CdTe QD sublayers have been grown with approximately the same thickness. In the multilayer films the number of LbL cycles per sublayer, that is, the sublayer thickness, was varied (see Figure 1b).

In Figure 2 the absorption spectra of the single component CdSe and CdTe films and a multilayer film with sublayers composed of 1 LbL cycle each are shown. The multilayer film exhibits the absorption features of both CdSe and CdTe QDs. The diamonds in Figure 2 represent the average of the absorbance of the single component CdSe and CdTe QD films. It can be seen that the multilayer absorbance is almost equal to the average of the absorbance of the single component films, which demonstrates that the LbL growth of multilayer and single component films is equally efficient. This is confirmed by film thickness measurements that show that the thickness of the film increases linearly with the number of dipping cycles and that each cycle leads to the deposition of 1−2

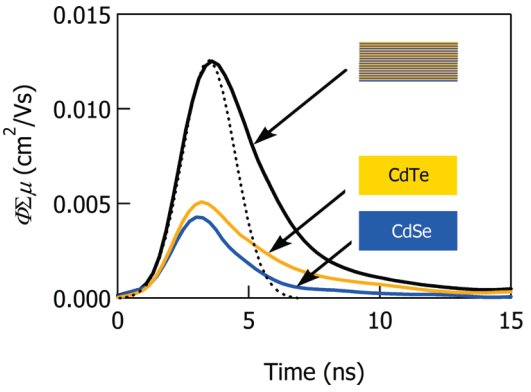

Figure 3. Typical TRMC transients of single component CdSe (yellow solid curve) and CdTe (blue solid curve) QD films and a multilayer film (black solid curve) composed of sublayers of 1 LbL cycle each. The excitation density corresponds to 0.1 absorbed photons/QD. The temporal shape of the laser pulse used to photoexcite the samples is shown as the black dotted curve.

monolayers of QDs. The absorption features of the films are broader than those of the respective QDs dispersed in solution, which is generally observed when the interparticle distance is reduced and is often attributed to enhanced electronic coupling or to disorder in the film.[14,15,29,30] The position of the first excitonic peak is only slightly red-shifted, which excludes significant particle growth during the LbL treatment.[7]

The photoconductivity of the films was measured using the time-resolved microwave conductivity (TRMC technique (see Experimental Section for details). Typical photoconductivity transients of the single component QD films and a multilayer film grown with 1 LbL cycle per sublayer are shown in Figure 3. The samples were photoexcited at 530 nm, where both the CdSe and CdTe QDs absorb (see Figure 2). The photoconductivity increases due to charge generation during the laser pulse and reaches a maximum as a result of the balance of charge generation and decay during the pulse. Subsequently, the photoconductivity decays due to charge recombination or trapping. The measured decay curve is the result of the convolution of the photoconductivity decay and the temporal shape of the photoexcitation laser pulse (dotted curve on Figure 2). We can fit the measured traces to the convolution of the laser pulse shape and a single exponential decay with a lifetime of 5−10 ns. Since the charge carrier lifetime is close to the laser pulse duration (3 ns) the uncertainty in determining the lifetime is large and detailed insight into the decay kinetics cannot be obtained. The maximum of the photoconductivity signal is used to calculate the product $\Phi_0\Sigma\mu$, where Φ_0 is the yield for charge carrier photogeneration per absorbed photon and $\Sigma\mu$ is the sum of the electron and hole mobilities. The photoconductivity is very similar for the single component films of CdSe and CdTe QDs with a $\Phi_0\Sigma\mu$ product of approximately 5×10^{-3} cm^2/(V s) (Figure 3, blue and yellow curves). As a result of charge carrier decay during the laser pulse Φ_0 is lower than 1, which implies that $\Sigma\mu$ is higher than 5×10^{-3} cm^2/(V s). From Figure 3 it can be seen that the product of the charge carrier photogeneration yield and the sum of the carrier mobility for the multilayer film (Figure 3, black curve) is about three times higher than for the single component films.

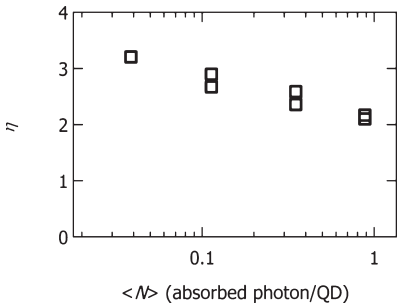

Figure 4. Photoconductivity enhancement with respect to the single component QD films for multilayer films with 1 LbL cycle per sublayer as a function of average excitation density. Different data points at the same excitation density are for different samples.

To compare the single component films and the multilayer films, we define the *photoconductivity enhancement* η as the ratio between the $\Phi_0\Sigma\mu$ product of the multilayer films ($\Phi_0\Sigma\mu_{\text{multilayer}}$) and that of the single component CdSe and CdTe QD films ($\Phi_0\Sigma\mu_{\text{CdSe}}$ and $\Phi_0\Sigma\mu_{\text{CdTe}}$) weighted by their relative absorptance at the excitation wavelength ($F_{\text{a CdSe}}$ and $F_{\text{a CdTe}}$):

$$\eta = \frac{\Phi_0 \sum_{\text{multilayer}} \mu \quad (F_{\text{a CdSe}} + F_{\text{a CdTe}})}{\Phi_0 \sum_{\text{CdSe}} \mu \, F_{\text{a CdSe}} + \Phi_0 \sum_{\text{CdTe}} \mu \, F_{\text{a CdTe}}}$$

Figure 4 shows the influence of excitation density, expressed as the average number of absorbed photons per QD, $\langle N \rangle$, on the photoconductivity enhancement for multilayer films with 1 LbL cycle per sublayer. The dependence of η on $\langle N \rangle$ is very small, but η is slightly lower at high excitation density. It appears that higher-order charge carrier/exciton recombination during the laser pulse reduces η at high excitation densities. The photoconductivity enhancement is 3.2 at the lowest excitation density.

If the bulk band alignment is preserved for the QDs, a type II junction is formed at the interface between CdSe and CdTe QDs, as illustrated in Figure 1c.[31] CdSe and CdTe have comparable charge carrier effective masses[32] and the QDs used in this study have similar bandgap energies, so it is likely that quantum confinement shifts the energy of the electronic levels in a similar fashion in the CdSe and CdTe QDs, retaining a type II junction at their interface. This band alignment has been confirmed by the demonstration of electron

transfer to CdSe QDs and hole transfer to CdTe QDs in junctions consisting of CdSe and CdTe QDs with sizes similar to those used for this study.[24] The photoconductivity enhancement in our multilayer films can formally be due to a higher charge carrier mobility or to a larger density of charges. That is, either $\Sigma\mu$ or Φ_0 could be enhanced. However, it is unlikely that the charge carrier mobility is larger in the multilayer films than in the single component films: different types of QDs in the multilayer films create disorder in site energies that would rather decrease the mobility.[33] Disorder in site energy can be seen as the introduction of potential barriers and shallow traps in the film that hinder charge transport. Furthermore, some intermixing of CdSe and CdTe QDs in the multilayer films cannot be excluded and would further contribute to a disordered energy landscape and a reduced charge carrier mobility. If there were a significant difference in mobility between the CdSe and the CdTe QD sublayers, transfer of mobile charges from the low-mobility sublayer to the high-mobility sublayer could also result in an increase of the photoconductivity. However, the CdSe and CdTe QD layers have a very similar microwave photoconductivity (see Figure 3), are prepared with analogous experimental procedures, and consist of QDs with similar sizes and charge carrier effective masses. Therefore, we assume that the charge carrier mobilities in our CdSe and CdTe QD layers are also very close. This implies that transfer of mobile charge carriers across the CdSe/CdTe interface does not result in a significant change in photoconductivity. Consequently, we attribute the photoconductivity enhancement to a higher density of mobile charges in the multilayer films.

It is an interesting question whether the primary excitations in CdSe and CdTe QD films are mobile charges or bound excitons. If photoexcitation results in the direct generation of free charge carriers (*i.e.*, the quantum yield for charge carrier photogeneration is close to one, even in the single component films), the higher density of charges at the maximum of the TRMC transient in the multilayer films would be due to a longer (subnanosecond) lifetime of the mobile charges and a resulting higher maximum of the photoconductivity transient. Such an increase in the charge carrier lifetime could result from, for instance, spatial separation of electrons and holes. Alternatively, the increase in photoconductivity can result from photogenerated excitons that do not contribute to the photoconductivity in the single component films but dissociate into spatially separated mobile charges at the CdSe/CdTe QD interface; this would imply that in the single component CdSe and CdTe QD layers, the quantum yield for photogeneration of charges is much lower than one.

To investigate which of the above applies we have investigated the photoconductivity enhancement at

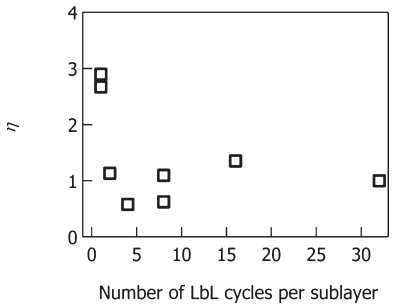

Figure 5. Photoconductivity enhancement with respect to the single component QD films for the multilayer films as a function of the number of LbL cycles per sublayer. The excitation density corresponds to 0.1 absorbed photons/QD. Different data points at the same number of LbL cycles per sublayer are for different samples.

different distances between the CdSe/CdTe interfaces. The number of LbL cycles per sublayer in the multilayer films has been varied to change the sublayer thickness (see Figure 1b). The distance that excitons/mobile charges have to diffuse in order to reach a CdSe/CdTe QD interface becomes shorter when the thickness of the sublayers is reduced. The photoconductivity enhancement η is plotted in Figure 5 as a function of the number of LbL cycles per sublayer. The photoconductivity of the multilayer films does not change significantly with respect to the single component films except for the thinnest sublayers (1 LbL cycle per sublayer), for which it improves by a factor of 3.

Thickness measurements of the LbL films showed that each cycle leads to the deposition of 1−2 monolayers of QDs. This suggests that in the multilayer films with 1 LbL cycle per sublayer all QDs are in contact, at least on one side, with a QD of another type. A very short diffusion length of the mobile charges or excitons that separate at the CdSe/CdTe QD interface could explain that only the multilayer films where all excitons/mobile charges are in direct contact with a dissociating interface, that is, the multilayer films with 1 LbL cycle per sublayer, show a clear enhancement. We can calculate a lower limit for the diffusion length d of the mobile charges from their lifetime (τ) of 5 ns and the lower limit for their mobility (μ) of 5×10^{-3} cm^2/(V s), as inferred from Figure 3. We use $d^2 = 6D\tau$, where the diffusion coefficient D is equal to $\mu(kT/e)$, where k is Boltzmann's constant, T is the temperature, and e is the electronic charge. This results in a diffusion length of at least 20 nm. Such a diffusion length is reasonable, as it has already been shown for similar CdSe and CdTe QDs systems that the charges are able to diffuse through several QD monolayers.[14,24] This suggests that if charges are the primary excitations in the QD films they would be able to reach the interface for sublayer thicknesses up to ~6 QDs. On the other hand, we find that the photoluminescence of the single component and the multilayer films is completely quenched (data not shown), which indicates that the exciton lifetime is

shorter than the 50 ps time resolution of our time-resolved photoluminescence setup. Such a short exciton lifetime implies a very short exciton diffusion length. While the above cannot be considered hard evidence, we tentatively conclude that the primary excitations in these Cd chalcogenide QD films are excitons and we attribute the photoconductivity enhancement in the multilayer films to exciton dissociation at the CdSe/CdTe interfaces.

Efficient exciton dissociation at the CdSe/CdTe QD interface requires that the exciton dissociation rate is higher than the exciton decay rate, which is at least $(50\ \text{ps})^{-1}$, based on the absence of detectable photoluminescence. For CdSe and CdTe QDs separated by 1 nm, a dissociation rate of at least $(1\ \text{ns})^{-1}$ was found,[34] and for CdSe–CdTe nanorod heterostructures the dissociation rate was on the order of $(1\ \text{ps})^{-1}$.[35] Since the QDs used in this study are separated by ligand molecules of only 0.4 nm (1,2-ethanediamine), which is intermediate between the two reported situations, a dissociation time on the order of tens of picoseconds is realistic. Since the yield for charge carrier photogeneration Φ_0 in the multilayer films is, by definition, at most one, and $\Phi_0\Sigma_i\mu$ of the multilayer films is more than three times higher than in the single component films, we conclude that the exciton dissociation yield in the single component CdSe and CdTe QD films is lower than 30%.

The absence of photoconductivity enhancement for the multilayer films with 2 LbL cycles per sublayers is surprising, as a significant fraction of excitons is photogenerated close to a CdSe/CdTe QD interface and should be able to dissociate. As discussed above, it is possible that disorder in site energy due to the presence of both CdSe and CdTe QDs in the multilayer films lowers the charge mobility. Consequently, the photoconductivity enhancement for the multilayer films that results from a larger density of mobile charges could be outweighed by a lower mobility due to disorder in the films.

In conclusion, films of coupled CdSe and CdTe QDs have been grown *via* a LbL process with a short 1,2-ethanediamine linker and show a comparable photoconductivity. The charge carriers have a lifetime on the order of nanoseconds and a mobility of at least $5 \times 10^{-3}\ \text{cm}^2/(\text{V s})$. Contact between CdSe and CdTe QDs in alternating layers leads to an increase of the photoconductivity by a factor of 3. Different scenarios for this enhancement are considered, and we conclude that exciton dissociation into mobile charges at the CdSe/CdTe interfaces is the most likely. Following this reasoning a yield for charge carrier photogeneration in single component CdSe or CdTe QD films of at most 30% is deduced. The photoconductivity was enhanced only for interfaces separated by 1–2 QD monolayers. This suggests that exciton diffusion in these CdSe and CdTe QD arrays is inefficient. Excitons that do not dissociate recombine nonradiatively to the ground state, as is inferred from the total quenching of the photoluminescence. Our results suggest that heterojunctions based on cadmium–chalcogenide QDs require an intimate contact between the different components, and that this can be achieved in layer-by-layer grown systems.

EXPERIMENTAL SECTION

All experiments were carried under N_2 atmosphere and anhydrous solvents were used.

Quantum Dot Synthesis. CdSe QDs were synthesized following the "green" recipe of Talapin *et al.*[36] Particle growth for 40 min results in ~3 nm-diameter QDs, as inferred from optical absorption measurements.[7] The QDs are stabilized by a combination of tri-*n*-octylphosphine oxide, hexadecylamine, and *n*-tetradecylphosphonic acid ligand molecules. The CdSe QDs were precipitated with methanol, centrifuged, and dispersed in toluene. After repeating the latter procedure three times to remove free surfactant molecules from the solution, the QDs were dispersed in chloroform.

Oleic acid (OA)-capped CdTe QDs were produced according to the synthesis developed by Kloper *et al.*[37] with small modifications. Squalane was preferred to octadecene because of its higher boiling point. The Te precursor solution was prepared by dissolving 0.128 g of Te in 2.5 mL of trioctylphosphine until the solution attained a clear, yellowish color. The solution was further diluted with squalane to a total volume of 5 mL. The Cd precursor solution was prepared by mixing 0.256 g of CdO with 2 mL of OA and 20 mL of squalane. The Cd solution was heated to 100 °C for 30 min under vacuum. Next, the system was flushed with N_2 gas and the temperature was raised to 300 °C, leading to formation of a homogeneous transparent solution and the generation of $Cd(OA)_2$. Further heating to 310 °C, for a period of about 30 min, led to the formation of a greyish precipitate attributed to the formation of Cd^0 nanoparticles.[37] The TOP/Te precursor solution was injected between 1 and 2 min after the appearance of the gray precipitate. The reaction mixture was cooled to room temperature 2 min after injection, resulting in ~4 nm QDs, as inferred from optical absorption measurements.[7] The reaction mixture was centrifuged in order to precipitate the crystalline Cd^0 nanoparticles and to separate them from the CdTe QD solution. The QDs were precipitated with a 1:1 v ethanol/acetone mixture, centrifuged, dispersed in toluene, and filtered with a 0.2 μm syringe filter. The QDs were precipitated again with ethanol, centrifuged, and finally dispersed in chloroform.

Film Preparation. QD films were prepared *via* a layer-by-layer (LbL) growth procedure[15,26] using a mechanical dip coater (DC Multi-8, Nima Technology) mounted inside a nitrogen glovebox. One LbL cycle consists in the successive dipping of a 1×0.5 in. quartz substrate into a QD solution in chloroform, a solution of 1,2-ethanediamine (EDA) in methanol, and a methanol rinsing solution (see Figure 1a). The single component CdSe or CdTe QD films as well as the multilayer films were grown by 32 dip cycles. All multilayer films consist of 16 cycles of CdSe QDs and 16 cycles of CdTe QDs, that is, 32 cycles in total, but the thickness of the CdSe and CdTe sublayers was varied by changing the alternating sequence of CdSe and CdTe cycles (see Figure 1b). The LbL growth conditions, such as dipping times, EDA concentration, and stirring of the solutions, were empirically optimized, and the conditions resulting in the highest film photoconductivity were selected. The EDA concentration was 10% v in methanol, the dipping time in the EDA and

rinsing solutions was 30 s for CdSe QD layers and 60 s for CdTe QD layers, and the rinsing solution was stirred for the CdSe QD layers. To avoid mixing of solvents, a drying step of 30 s was introduced between dipping into the QD solution and the EDA solution, and between dipping into the rinsing solution and the QD solution.

Characterization. The thickness of the films was measured with a Veeco Dektak 8 step-profilometer. Optical absorption spectra were recorded with a Perkin-Elmer Lambda 900 spectrometer equipped with an integrating sphere. The spectra were corrected for scattering and reflection by first placing the film at the entrance of the integrating sphere to obtain the transmittance F_t, and subsequently behind the integrating sphere to obtain the reflectance F_r. The absorptance was obtained as $F_a = 1 - F_r - F_t$ and the absorbance as $A = -\log(F_t/(1 - F_r))$. A Lifespec-ps setup using a 405 nm excitation source (Edinburgh instrument) was used for photoluminescence measurements.

The photoconductivity was investigated using the time-resolved microwave conductivity (TRMC) technique.[14,15,38] The samples were mounted in an open reflection cell. Photoexcitation laser pulses of 3 ns duration with a wavelength of 530 nm were obtained by pumping an optical parametric oscillator with the third harmonic of a Q-switched Nd:YAG laser (Opotek Vibrant 355 II). The photon flux I_0 was varied between 10^{14} and 3×10^{15} photons/cm^2/pulse, using neutral density filters. The average number of photons absorbed per QD is obtained as $\langle N \rangle = I_0\sigma$ where σ is the absorption cross section taken from ref 7. Upon photoexcitation the change in microwave power reflected from the cavity was measured. The change in reflected microwave power can be due to a change in the real and/or the imaginary component of the conductance of the sample. Here the imaginary component of the photoconductance was negligible compared to the real component. For small photoinduced changes in the real conductance of the sample, $\Delta G(t)$, and negligible change in imaginary conductance, the relative change in microwave power is

$$\frac{\Delta P(t)}{P} = -K\Delta G(t)$$

K is a sensitivity factor which has been determined previously.[39] The photoconductance $\Delta G(t)$ can be expressed as

$$\Delta G(t) = e\beta I_0 F_a \Phi(t) \Sigma\mu$$

where e is the elementary charge, β is the ratio between the broad and narrow inner dimensions of the waveguide, F_a is the absorptance of the sample, $\Phi(t)$ is the number of mobile charge carriers at time t per absorbed photon, and $\Sigma\mu$ is the sum of the electron and hole mobilities. For more details on the TRMC technique the reader is referred to refs 14, 15, and 38.

Acknowledgment. This work is part of SELECT—Silicon Based Superlattices with Spectrum Selective Absorbers. SELECT is financed by SenterNovem; program: `Energie Onderzoek Subsidie: Lange Termijn'. The 3TU Centre for Sustainable Energy Technologies is acknowledged for financial support. A.J.H. acknowledges financial support by the Dutch Foundation of Scientific Research (NWO) through a NWO-VENI grant.

REFERENCES AND NOTES

1. Alivisatos, A. P. Perspectives on the Physical Chemistry of Semiconductor Nanocrystals. *J. Phys. Chem.* **1996**, *100*, 13226–13239.
2. Roduner, E. Size Matters: Why Nanomaterials Are Different. *Chem. Soc. Rev.* **2006**, *35*, 583–592.
3. Vanmaekelbergh, D.; Liljeroth, P. Electron-Conducting Quantum Dot Solids: Novel Materials Based on Colloidal Semiconductor Nanocrystals. *Chem. Soc. Rev.* **2005**, *34*, 299–312.
4. Donega, C. D.; Liljeroth, P.; Vanmaekelbergh, D. Physicochemical Evaluation of the Hot-Injection Method, a Synthesis Route for Monodisperse Nanocrystals. *Small* **2005**, *1*, 1152–1162.
5. Murray, C. B.; Sun, S. H.; Gaschler, W.; Doyle, H.; Betley, T. A.; Kagan, C. R. Colloidal Synthesis of Nanocrystals and Nanocrystal Superlattices. *IBM J. Res. Dev.* **2001**, *45*, 47–56.
6. Qu, L. H.; Peng, Z. A.; Peng, X. G. Alternative Routes toward High Quality CdSe Nanocrystals. *Nano Lett.* **2001**, *1*, 333–337.
7. Yu, W. W.; Qu, L. H.; Guo, W. Z.; Peng, X. G. Experimental Determination of the Extinction Coefficient of CdTe, CdSe, and CdS Nanocrystals. *Chem. Mater.* **2003**, *15*, 2854–2860.
8. Donega, C. D.; Koole, R. Size Dependence of the Spontaneous Emission Rate and Absorption Cross Section of CdSe and CdTe Quantum Dots. *J. Phys. Chem. C* **2009**, *113*, 6511–6520.
9. Efros, A. L.; Rosen, M.; Kuno, M.; Nirmal, M.; Norris, D. J.; Bawendi, M. Band-Edge Exciton in Quantum Dots of Semiconductors with a Degenerate Valence Band: Dark and Bright Exciton States. *Phys. Rev. B* **1996**, *54*, 4843–4856.
10. Koole, R.; Allan, G.; Delerue, C.; Meijerink, A.; Vanmaekelbergh, D.; Houtepen, A. J. Optical Investigation of Quantum Confinement in PbSe Nanocrystals at Different Points in the Brillouin Zone. *Small* **2008**, *4*, 127–133.
11. Liu, Y.; Gibbs, M.; Puthussery, J.; Gaik, S.; Ihly, R.; Hillhouse, H. W.; Law, M. Dependence of Carrier Mobility on Nanocrystal Size and Ligand Length in PbSe Nanocrystal Solids. *Nano Lett* **2010**, *10*, 1960–9.
12. Law, M.; Luther, J. M.; Song, O.; Hughes, B. K.; Perkins, C. L.; Nozik, A. J. Structural, Optical, and Electrical Properties of PbSe Nanocrystal Solids Treated Thermally or with Simple Amines. *J. Am. Chem. Soc.* **2008**, *130*, 5974–5985.
13. Yu, D.; Wehrenberg, B. L.; Jha, P.; Ma, J.; Guyot-Sionnest, P. Electronic Transport of N-Type CdSe Quantum Dot Films: Effect of Film Treatment. *J. Appl. Phys.* **2006**, *99*, 104315.
14. Talgorn, E.; Abellon, R. D.; Kooyman, P. J.; Piris, J.; Savenije, T. J.; Goossens, A.; Houtepen, A. J.; Siebbeles, L. D. A. Supercrystals of CdSe Quantum Dots with High Charge Mobility and Efficient Electron Transfer to TiO_2. *ACS Nano* **2010**, *4*, 1723–31.
15. Talgorn, E.; Moysidou, E.; Abellon, R. D.; Savenije, T. J.; Goossens, A.; Houtepen, A. J.; Siebbeles, L. D. A. Highly Photoconductive CdSe Quantum-Dot Films: Influence of Capping Molecules and Film Preparation Procedure. *J. Phys. Chem. C* **2010**, *114*, 3441–3447.
16. Houtepen, A. J.; Kockmann, D.; Vanmaekelbergh, D. Reappraisal of Variable-Range Hopping in Quantum-Dot Solids. *Nano Lett.* **2008**, *8*, 3516–3520.
17. Vanmaekelbergh, D.; Houtepen, A. J.; Kelly, J. J. Electrochemical Gating: A Method to Tune and Monitor the (Opto)Electronic Properties of Functional Materials. *Electrochim. Acta* **2007**, *53*, 1140–1149.
18. Roest, A. L.; Houtepen, A. J.; Kelly, J. J.; Vanmaekelbergh, D. Electron-Conducting Quantum-Dot Solids with Ionic Charge Compensation. *Faraday Discuss.* **2004**, *125*, 55–62.
19. Choi, J. J.; Lim, Y. F.; Santiago-Berrios, M. B.; Oh, M.; Hyun, B. R.; Sung, L. F.; Bartnik, A. C.; Goedhart, A.; Malliaras, G. G.; Abruna, H. D.; *et al.* Pbse Nanocrystal Excitonic Solar Cells. *Nano Lett.* **2009**, *9*, 3749–3755.
20. Pattantyus-Abraham, A. G.; Kramer, I. J. B., A. R.; Wang, X. H. K., G.; Debnath, R. L., L.; Raabe, I.; Nazeeruddin, M. K. G., M.; Sargent, E. H. Depleted-Heterojunction Colloidal Quantum Dot Solar Cells. *ACS Nano* **2010**, *4*, 3378–3380.
21. Zhao, N.; Osedach, T. P.; Chang, L.-Y.; Geyer, S. M.; Wanger, D.; Binda, M. T.; Arango, A. C.; Bawendi, M. G.; Bulovic, V. Colloidal PbS Quantum Dot Solar Cells with High Fill Factor. *ACS Nano* **2010**, *4*, 3743–3752.
22. Luther, J. M.; Law, M.; Beard, M. C.; Song, Q.; Reese, M. O.; Ellingson, R. J.; Nozik, A. J. Schottky Solar Cells Based on Colloidal Nanocrystal Films. *Nano Lett.* **2008**, *8*, 3488–3492.
23. Gur, I.; Fromer, N. A.; Geier, M. L.; Alivisatos, A. P. Air-Stable All-Inorganic Nanocrystal Solar Cells Processed from Solution. *Science* **2005**, *310*, 462–465.
24. Gross, D.; Mora-Sero, I.; Dittrich, T.; Belaidi, A.; Mauser, C.; Houtepen, A. J.; Da Como, E.; Rogach, A. L.; Feldmann, J. Charge Separation in Type II Tunneling Multilayered

Structures of CdTe and CdSe Nanocrystals Directly Proven by Surface Photovoltage Spectroscopy. *J. Am. Chem. Soc.* **2010**, *132*, 5981–5983.
25. Meulenberg, R. W.; Lee, J. R. I.; Wolcott, A.; Zhang, J. Z.; Terminello, L. J.; van Buuren, T. Determination of the Exciton Binding Energy in CdSe Quantum Dots. *ACS Nano* **2009**, *3*, 325–330.
26. Luther, J. M.; Law, M.; Song, Q.; Perkins, C. L.; Beard, M. C.; Nozik, A. J. Structural, Optical and Electrical Properties of Self-Assembled Films of PbSe Nanocrystals Treated with 1,2-Ethanedithiol. *ACS Nano* **2008**, *2*, 271–280.
27. Olsson, Y. K.; Chen, G.; Rapaport, R.; Fuchs, D. T.; Sundar, V. C.; Steckel, J. S.; Bawendi, M. G.; Aharoni, A.; Banin, U. Fabrication and Optical Properties of Polymeric Waveguides Containing Nanocrystalline Quantum Dots. *Appl. Phys. Lett.* **2004**, *85*, 4469–4471.
28. The length of the molecule was estimated from the molecule geometries optimized using the semi-emperical method AM1 in Spartan `02.
29. Dollefeld, H.; Weller, H.; Eychmuller, A. Particle−Particle Interactions in Semiconductor Nanocrystal Assemblies. *Nano Lett.* **2001**, *1*, 267–269.
30. Artemyev, M. V.; Woggon, U.; Jaschinski, H.; Gurinovich, L. I.; Gaponenko, S. V. Spectroscopic Study of Electronic States in an Ensemble of Close-Packed CdSe Nanocrystals. *J. Phys. Chem. B* **2000**, *104*, 11617–11621.
31. Chiang, T. C.; Himpsel, F. J.; Goldmann, A.; Koch, E.-E. *SpringerMaterials—The Landolt−Börnstein Database*: Springer.
32. Kasap, S.; Capper, P., Eds. *Springer Handbook of Electronic and Photonic Materials*. Springer: New York, 2006.
33. Chandler, R. E.; Houtepen, A. J.; Nelson, J.; Vanmaekelbergh, D. Electron Transport in Quantum Dot Solids: Monte Carlo Simulations of the Effects of Shell Filling, Coulomb Repulsions, and Site Disorder. *Phys. Rev. B* **2007**, *75*, 085325.
34. Gross, D.; Susha, A. S.; Klar, T. A.; Da Como, E.; Rogach, A. L.; Feldmann, J. Charge Separation in Type II Tunneling Structures of Close-Packed CdTe and CdSe Nanocrystals. *Nano Lett.* **2008**, *8*, 1482–1485.
35. Scholes, G. D.; Jones, M.; Kumar, S. Energetics of Photoinduced Electron-Transfer Reactions Decided by Quantum Confinement. *J. Phys. Chem. C* **2007**, *111*, 13777–13785.
36. Mekis, I.; Talapin, D. V.; Kornowski, A.; Haase, M.; Weller, H. One-Pot Synthesis of Highly Luminescent CdSe/CdS Core−Shell Nanocrystals *via* Organometallic and "Greener" Chemical Approaches. *J. Phys. Chem. B* **2003**, *107*, 7454–7462.
37. Kloper, V.; Osovsky, R.; Kolny-Olesiak, J.; Sashchiuk, A.; Lifshitz, E. The Growth of Colloidal Cadmium Telluride Nanocrystal Quantum Dots in the Presence of Cd^0 Nanoparticles. *J. Phys. Chem. C* **2007**, *111*, 10336–10341.
38. Kroeze, J. E.; Savenije, T. J.; Warman, J. M. Electrodeless Determination of the Trap Density, Decay Kinetics, and Charge Separation Efficiency of Dye-Sensitized Nanocrystalline TiO_2. *J. Am. Chem. Soc.* **2004**, *126*, 7608–7618.
39. Savenije, T. J.; de Haas, M. P.; Warman, J. M. The Yield and Mobility of Charge Carriers in Smooth and Nanoporous TiO_2 Films. *Z. Phys. Chem.* **1999**, *212*, 201–206.